Research Square

Preprints are preliminary reports that have not undergone peer review.
They should not be considered conclusive, used to inform clinical practice,
or referenced by the media as validated information.

LGALS3BP in liver cirrhosis: a genetic-based discovery from platelet-related genes with predictive diagnostic value

Shanshan Huan
The First Affiliated Hospital of Fujian Medical University
Yupeng Chen
The First Affiliated Hospital of Fujian Medical University
Huinan Lu
The First Affiliated Hospital of Fujian Medical University
Xiaodan Fu
1002603440@qq.com

The First Affiliated Hospital of Fujian Medical University

Article

Keywords: LGALS3BP, Liver cirrhosis, Thrombocytopenia, Diagnostic model, Immune microenvironment

Posted Date: April 1st, 2026

DOI: https://doi.org/10.21203/rs.3.rs-8835847/v1

License: This work is licensed under a Creative Commons Attribution 4.0 International License.
Read Full License

Additional Declarations: No competing interests reported.

LGALS3BP in liver cirrhosis: a genetic-based discovery from platelet-related genes with predictive diagnostic value

Shanshan Huan[1], Yupeng Chen[1], Huinan Lu[1], Xiaodan Fu[1]*

Abstract

Background: Thrombocytopenia, a major complication of liver cirrhosis, elevates bleeding risk and worsens patient prognosis, especially after invasive procedures. Despite its clinical significance, the molecular mechanisms underpinning platelet dysfunction in cirrhosis remain elusive.

Methods: We conducted an integrative analysis to define the diagnostic value of platelet-related genes in cirrhosis and to decipher platelet-liver cell interactions. Bioinformatics approaches were applied to public datasets to identify key genes and construct a receiver operating characteristic (ROC)-based diagnostic model, with validation in multiple independent cohorts. Functional enrichment and immune infiltration analyses were performed. Findings were experimentally validated using qRT-PCR and immunohistochemistry in clinical samples.

Results: We established a robust platelet-related gene diagnostic model and identified LGALS3BP as a high-value diagnostic biomarker for liver cirrhosis. Groups with high and low LGALS3BP expression exhibited distinct biological functions and immune microenvironment profiles, suggesting an immunomodulatory role in disease progression. Crucially, in vitro functional studies demonstrated that LGALS3BP acts as a key molecular mediator linking hepatic fibrosis to platelet activation.

Conclusion: This study identifies LGALS3BP as a pivotal molecular link in cirrhotic thrombocytopenia and establishes a novel diagnostic model based on platelet-related genes. Our findings highlight LGALS3BP's role in mediating platelet-liver cell crosstalk and its association with the immune microenvironment, providing new insights into disease progression. This work not only advances the molecular understanding of liver cirrhosis but also offers a promising diagnostic tool with potential clinical utility.

---

[1]Department of pathology,The First Affiliated Hospital of Fujian Medical University,No.20,Chazhong Road, Fuzhou, Fujian, 350004, P.R. China

This research was partially supported by the National Clinical Specialization Construction Project for the Department of Pathology(Progressive project)(2022YBL-JB-01).

The authors declare no conflict of interest or financial ties to disclose.

* corresponding author: Xiaodan Fu Department of pathology,The First Affiliated Hospital of Fujian Medical University,No.20,Chazhong Road, Fuzhou, Fujian, 350004, P.R.China(emailaddress:1002603440@qq.com)

Keywords

LGALS3BP ; Liver cirrhosis; Thrombocytopenia; Diagnostic model; Immune microenvironment

Introduction

Liver cirrhosis is a chronic pathological condition characterized by structural remodeling of the liver due to prolonged injury and fibrosis. It typically develops from hepatic fibrosis, which results from excessive accumulation of extracellular matrix (ECM) following chronic hepatic injury caused by viral infections, alcohol abuse, nonalcoholic fatty liver disease, or chemical damage [1,2]. Cirrhosis is also one of the most common precursors of hepatocellular carcinoma [4]. Although antifibrotic drugs have been explored in animal models [5], few have been successfully translated into clinical use. Therefore, elucidating the pathogenesis of cirrhosis and identifying novel therapeutic targets remain urgent challenges.

Most patients with liver cirrhosis exhibit thrombocytopenia and platelet dysfunction. Thrombocytopenia increases bleeding risk and is closely associated with postoperative hemorrhage after invasive procedures. Thus, managing thrombocytopenia is essential for improving clinical outcomes in cirrhotic patients. In recent years, increasing evidence has shown that platelets act not only as effector cells but also as immune modulators that influence tumor progression [6,8]. Given that the liver is a highly vascularized organ and thrombocytopenia is common in cirrhosis, we hypothesized that platelets might interact with hepatic cells through specific molecular crosstalk mechanisms that affect disease progression.

Existing studies have primarily focused on platelet counts, platelet function, and surgical risk assessment in cirrhosis [7,11], with few investigating the molecular pathways involving platelet-related genes. To explore the predictive and diagnostic potential of platelet-related genes in liver cirrhosis, we conducted bioinformatics analyses using publicly available datasets to identify key genes, construct an ROC-based diagnostic model, and validate it in multiple independent datasets. Additionally, we analyzed biological and immune differences between high- and low-expression cirrhosis groups. Paraffin-embedded tissue samples from cirrhotic patients with thrombocytopenia were further examined using qRT-PCR and immunohistochemistry to validate the bioinformatics results. However, whether the identified target gene mediates platelet-induced hepatic fibrosis or regulates platelet activation in hepatic stellate cells requires further investigation through co-culture and animal experiments. Our findings reveal gene-level associations between platelets and cirrhotic cells, suggesting potential diagnostic utility and providing novel insights for therapeutic target discovery.

Materials and Methods

Data Collection and Processing

RNA-seq datasets of cirrhotic and normal liver tissues were obtained from the Gene Expression Omnibus (GEO) database (http://www.ncbi.nlm.nih.gov/geo/). The GSE89377 dataset was used as the training set. Perl scripts were used to convert Ensembl IDs in the raw expression matrix to corresponding gene symbols, and the expression values (FPKM) were converted to TPM for further analyses. GSE14323 and GSE139602 datasets were used as validation sets. A total of 620 platelet-related genes (PRGs) involved in platelet activation, adhesion, aggregation, and signal transduction were extracted from the MSigDB database (http://www.broad.mit.edu/gsea/msigdb/).

Identification and Functional Analysis of Differentially Expressed Platelet-Related Genes

Differential expression analysis between cirrhosis and control samples in GSE89377 was performed using the limma R package (version 3.40.6), with a significance threshold of $P < 0.05$.

Median absolute deviation (MAD) values were calculated for each gene, and the lowest 50% were removed. The WGCNA R package was used to construct a weighted gene co-expression network after removing outlier genes and samples via the *goodSamplesGenes* method. Eleven co-expression modules were identified, and the yellow module showing the strongest correlation with cirrhosis was selected for further analysis.

Venn diagram analysis was performed among DEGs from GSE89377, genes from the significant WGCNA module, and PRGs to identify 42 differentially expressed platelet-related genes (DEPRGs).

Functional enrichment analyses of DEPRGs were conducted using GO and KEGG, while protein–protein interaction (PPI) networks were constructed using the STRING database (https://string-db.org/).

Selection of Candidate Genes

Based on the DEPRGs identified, LASSO regression analysis was performed to select representative genes, followed by Random Forest analysis. The intersection of genes from both methods was determined using a Venn diagram to identify the final candidate genes.

Construction and Validation of the Platelet Diagnostic Model

Five candidate genes were used to construct a diagnostic model using the glmnet R package. Survival time, survival status, and gene expression data were integrated, and threefold cross-validation was employed to determine the optimal model parameters.

ROC curves and the area under the curve (AUC) were used to evaluate the model's diagnostic accuracy via the timeROC package. External validation was performed using the GSE14323 and GSE139602 datasets to confirm the model's stability and reliability.

Pathway Analysis

Gene Set Enrichment Analysis (GSEA, version 3.0) was performed to identify pathways associated with high and low expression groups of the five candidate genes. The *c2.cp.kegg.v7.4.symbols.gmt* subset from the Molecular Signatures Database (http://www.gsea-msigdb.org/gsea/downloads.jsp) was used for enrichment analysis based on gene expression profiles and phenotypic grouping.

Immune Infiltration Analysis

Based on the GSE89377 expression data, the IOBR R package was used to perform immune infiltration analysis with the CIBERSORT algorithm (DOI: 10.1038/nmeth.3337). Twenty-two immune cell subtypes were quantified for each sample, and the results were visualized using stacked bar plots, boxplots, and correlation heatmaps.

qRT-PCR

Total RNA was extracted from paraffin-embedded liver tissues of cirrhotic patients with thrombocytopenia (platelet count < 50 × 10^9/L) and non-cirrhotic controls using the *RNeasy Mini Kit* (Qiagen). Reverse transcription and quantitative real-time PCR (qRT-PCR) were performed using *QIAGEN* kits to evaluate the expression of the selected target genes PDK1, TFPI, TXLNG, SYTL4, and LGALS3BP. Relative expression levels were calculated using the $2^{-\triangle\triangle CT}$method.

Immunohistochemistry (IHC)

Tissue microarrays were constructed from paraffin-embedded cirrhotic and non-cirrhotic samples. Sections were stained with a mouse anti-human LGALS3BP antibody using standard immunohistochemical procedures. Platelet infiltration within the liver tissues was also examined.

Results

1. Identification of Differentially Expressed Platelet-Related Genes

Using the Limma package, a total of 446 DEGs were identified in the GSE89377 dataset, including 116 upregulated and 330 downregulated genes (Figures 1A and 1B).The WGCNA was then applied to identify modules most strongly associated with liver cirrhosis. A soft threshold of $\beta = 6$ was selected based on the analysis of scale

independence and mean connectivity (Figures 1C and 1D). The clustering dendrogram of samples from cirrhosis and control groups is shown in Figure 1E, and eleven distinct gene co-expression modules were identified, each represented by a unique color in the dendrogram (Figures 1F and 1G).The correlation between clinical traits and gene modules is illustrated in Figure 1H, revealing that the yellow module (comprising 592 genes) exhibited the strongest positive correlation with liver cirrhosis (correlation coefficient = 0.86, $P = 2.6 \times 10^{-8}$). Therefore, the yellow module was selected as the key module for subsequent analyses. Further evaluation demonstrated a significant positive correlation between the module eigengene and cirrhosis-related gene expression (r = 0.89, Figure 1I), confirming that the yellow module genes were most strongly associated with liver cirrhosis.

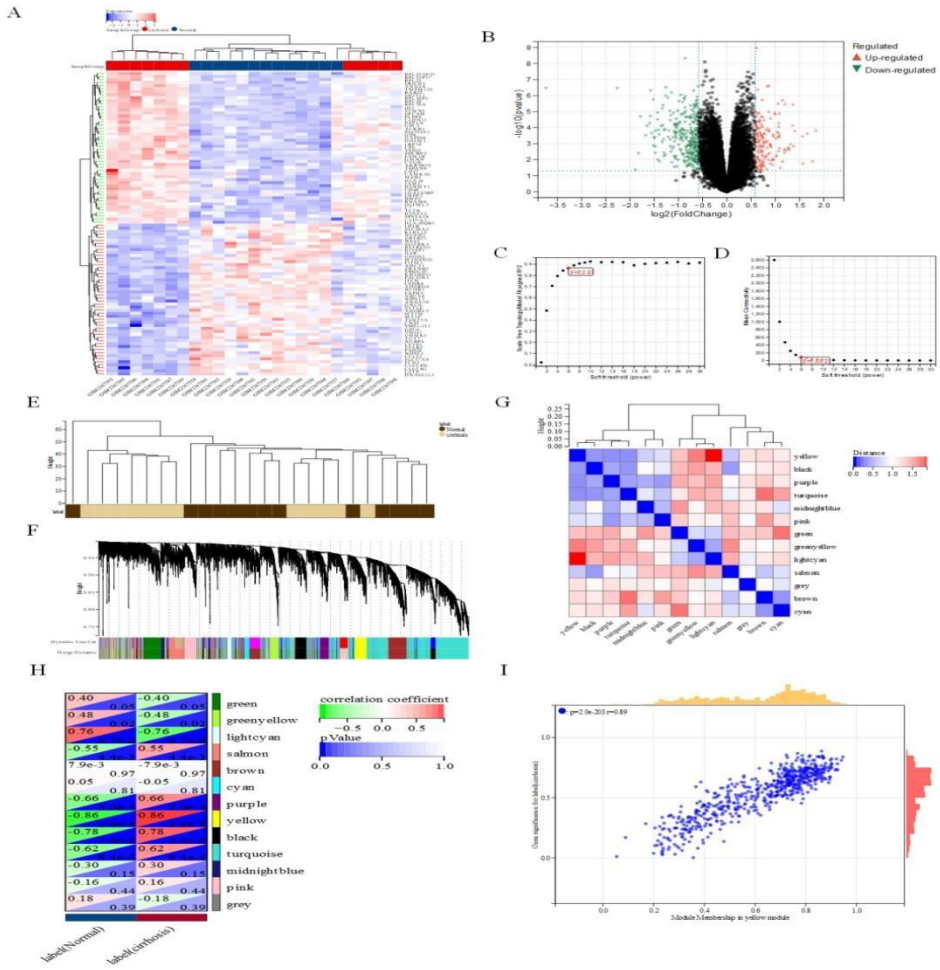


Figure 1. Identification of DEGs and Module Genes in Liver Cirrhosis Using Limma and WGCNA

(A) Heatmap showing the top 50 upregulated and downregulated DEGs identified in liver cirrhosis. Red and blue represent upregulated and downregulated gene expression, respectively.

(B) Volcano plot illustrating all DEGs, where red and green denote significantly upregulated and downregulated genes, respectively.

(C, D) Determination of the soft-thresholding power (β = 6) based on scale independence and mean connectivity analyses.

(E) Sample clustering dendrogram of cirrhosis and control groups.

(F) Gene dendrogram showing 11 distinct co-expression modules, each labeled with a different color.
(G) Heatmap of module eigengenes.
(H) Heatmap depicting correlations between gene modules and liver cirrhosis. The yellow module showed the strongest positive correlation with cirrhosis; the numbers in each cell represent the correlation coefficient and *P*-value.
(I) Scatter plot showing the correlation between module membership and gene significance for genes in the yellow module.

2. **Functional Analysis of Differentially Expressed Platelet-Related Genes**

A Venn analysis (Figure 2A) was performed to identify overlapping genes among the 446 DEGs (identified by Limma), the 592 genes in the WGCNA yellow module, and the platelet-related gene set (PRGs). This intersection yielded 42 differentially expressed platelet-related genes (DEPRGs) between cirrhotic and normal control samples.

Functional enrichment analyses of the DEPRGs were conducted using KEGG and GO annotations.KEGG analysis revealed that DEPRGs were mainly enriched in pathways including platelet activation, axon guidance, focal adhesion, AGE–RAGE signaling, and the HIF-1 signaling pathway (Figure 2B).GO analysis indicated that DEPRGs were primarily enriched in biological processes (BP) related to extracellular secretion regulation, coagulation, hemostasis, platelet degranulation, and platelet activation (Figure 2C).In the cellular component (CC) category, DEPRGs were enriched in the extracellular region, extracellular space, secretory granule, platelet alpha granule, cytoplasmic vesicle lumen, and collagen-containing extracellular matrix (Figure 2D).In the molecular function (MF) category, enrichment was observed in signal receptor binding, transferase activity, endopeptidase inhibitor activity, and integrin binding (Figure 2E).Overall, these functional enrichment results indicate that the DEPRGs are mainly involved in platelet activation, immune response, inflammatory regulation, and extracellular matrix organization, processes that are closely associated with the pathogenesis of thrombocytopenia in liver cirrhosis. These findings provide a reliable foundation for subsequent analyses.

In addition, a PPI network of DEPRGs was constructed to identify key interacting hub genes. The resulting PPI network (Figure 2F) revealed 11 genes with strong

interconnections, suggesting potential cooperative regulatory relationships among these platelet-related genes in liver cirrhosis.

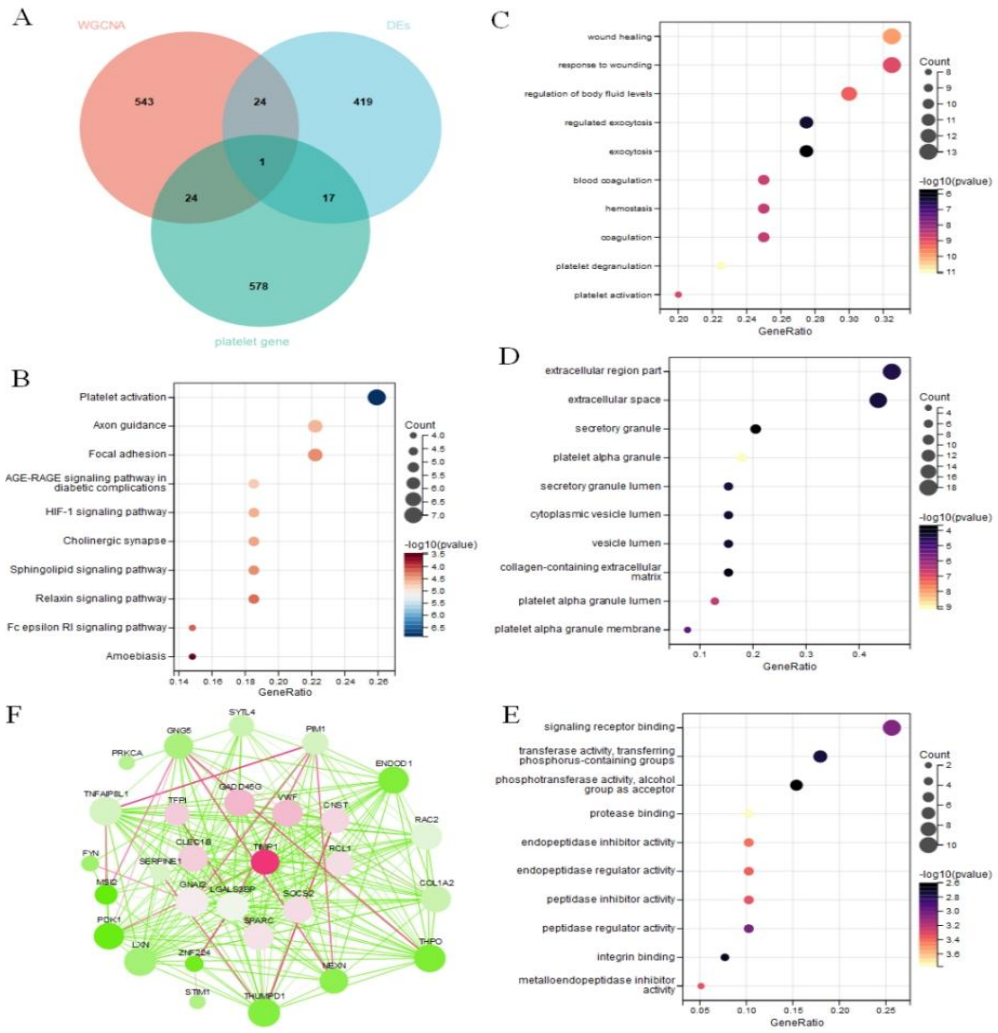


Figure 2. Identification and Functional Analysis of Differentially Expressed Platelet-Related Genes

(A) Venn diagram showing the overlap among DEGs identified by Limma, genes from the WGCNA yellow module, and platelet-related genes (PRGs), resulting in 42 differentially expressed platelet-related genes (DEPRGs).

(B) KEGG pathway enrichment analysis of DEPRGs.

(C–E) GO enrichment analysis, including biological processes (BP), cellular components (CC), and molecular functions (MF).

(F) PPI network analysis of DEPRGs.

3. Identification of Differentially Expressed Platelet-Related Candidate Genes

To further screen candidate genes with diagnostic potential, the 42 DEPRGs were analyzed using LASSO-Cox regression and Random Forest algorithms. LASSO-Cox regression identified 10 potential diagnostic markers (Figures 3A, B), while Random Forest analysis identified 14 candidate genes ranked by importance scores (Figure

3C). The intersection of these two gene sets, determined through Venn analysis, yielded five candidate diagnostic genes: PDK1, TFPI, TXLNG, SYTL4, and LGALS3BP (Figure 3D).

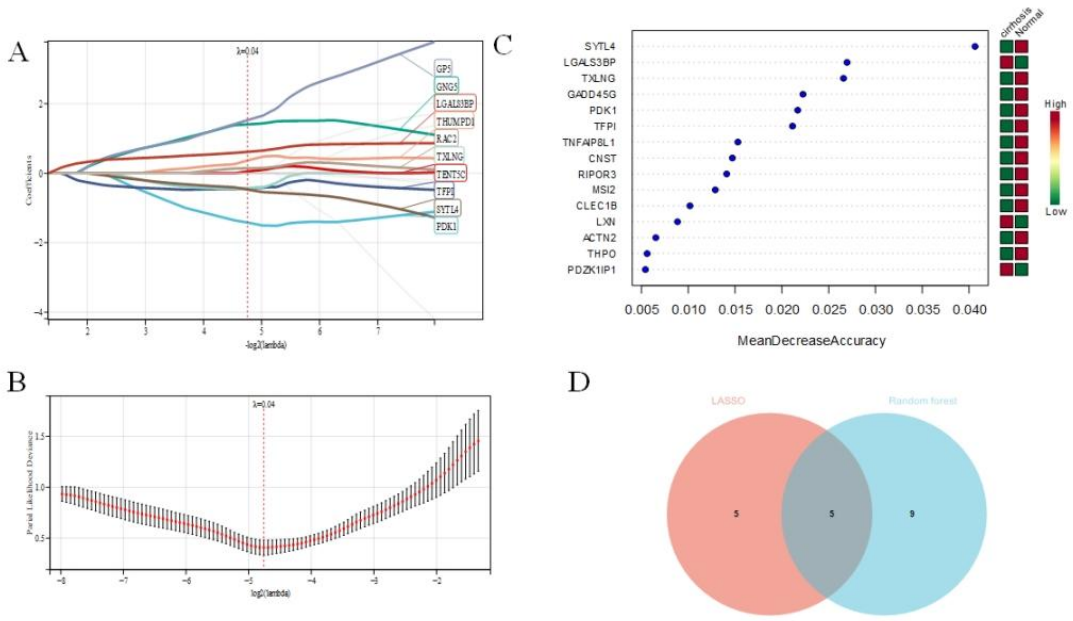


Figure 3. Screening of Platelet-Related Diagnostic Biomarkers for Liver Cirrhosis

(A, B) LASSO-Cox regression identified 10 diagnostic markers, with the lowest point on the curve (n=5) indicating the optimal model.

(C) Random Forest analysis identified 14 diagnostic genes ranked by importance.

(D) Venn diagram showing five overlapping candidate diagnostic genes identified by both algorithms.

4. Construction and Validation of the Platelet-Related Diagnostic Model

Boxplots revealed differential expression of the five candidate genes across the training dataset GSE89377 (Figure 4A) and validation datasets GSE14323 (Figure 4G) and GSE139602 (Figure 4J). A ROC-based diagnostic model was then established to evaluate the specificity and sensitivity of these genes. The AUC values for PDK1, TFPI, TXLNG, SYTL4, and LGALS3BP were 0.93, 0.94, 0.93, 0.91, and 0.94,respectively (Figures 4B–F).In the validation dataset GSE14323, LGALS3BP and TFPI achieved AUCs of 1.0 and 0.9 (Figures 4H, I), while in GSE139602, LGALS3BP reached an AUC of 0.97 (Figure 4K). These findings demonstrate that

LGALS3BP exhibits strong diagnostic potential for liver cirrhosis.

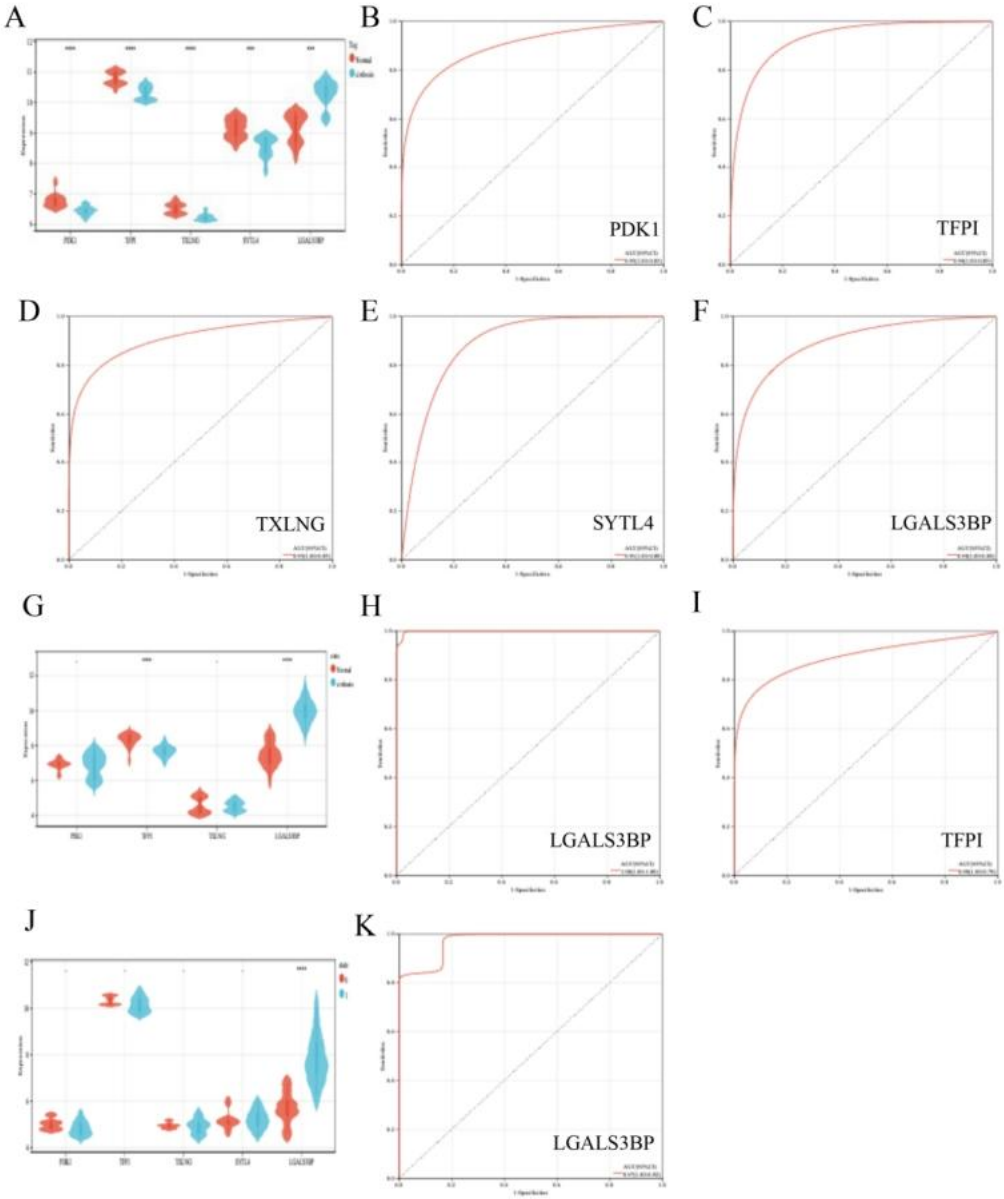


Figure 4. Construction and Validation of the Diagnostic Model

(A) Expression analysis of the five candidate genes (PDK1, TFPI, TXLNG, SYTL4, LGALS3BP) in the training dataset.

(B–F) ROC curves for the five-gene diagnostic model demonstrating robust predictive value.

(G–I) Expression and ROC analyses of candidate genes in the GSE14323 validation dataset.

(J–K) Expression and ROC analyses in the GSE139602 validation dataset.

5. Pathway Analysis

To elucidate the potential pathways and molecular mechanisms associated with the five candidate genes, GSEA was performed based on gene expression profiles and phenotype grouping.PDK1 was enriched in the Hedgehog signaling pathway,

autoimmune thyroid disease, small-cell lung cancer, and spliceosome (Figure 5A).TFPI was associated with cell adhesion molecules (CAMs), leukocyte transendothelial migration, and primary immunodeficiency (Figure 5B).TXLNG was enriched in the VEGF signaling pathway, melanoma, cell adhesion molecules, and Fc epsilon RI signaling (Figure 5C).SYTL4 was enriched in pathways related to ganglioside biosynthesis, cardiac muscle contraction, and ribosome and metabolic synthesis (Figure 5D).LGALS3BP was enriched in biosynthesis and metabolic processes, ECM–receptor interaction, lysine degradation, and gap junctions (Figure 5E).

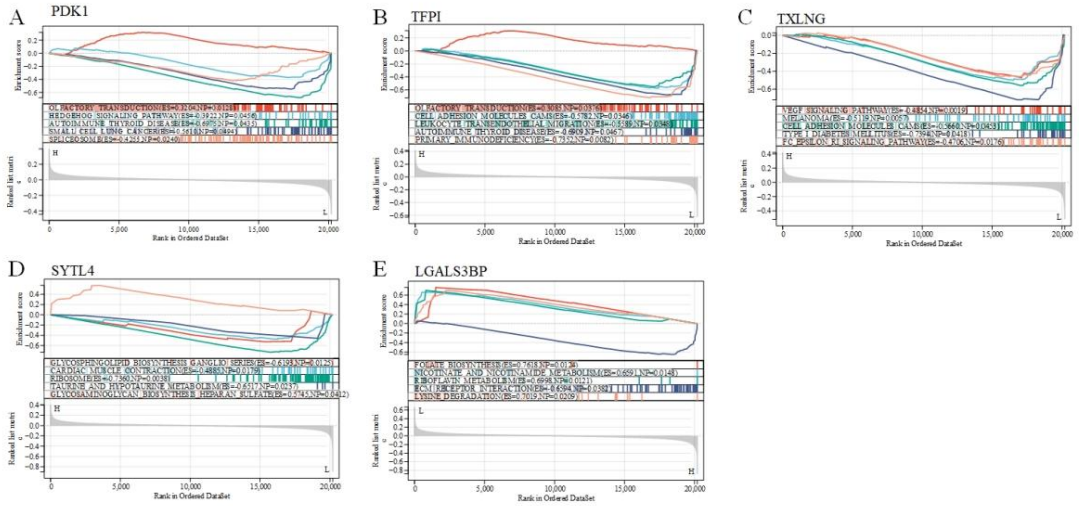


Figure 5. GSEA of Candidate Genes Between Cirrhotic and Control Groups

(A–E) Pathway enrichment analyses of the five candidate genes (PDK1, TFPI, TXLNG, SYTL4, LGALS3BP).

6. Immune Infiltration Analysis

CIBERSORT, a deconvolution algorithm for estimating immune cell composition, revealed significant differences in plasma cells, $CD4^+$ memory T cells, and macrophages between cirrhotic and control samples ($P < 0.05$) (Figure 6A-C).PDK1, TFPI, TXLNG, and SYTL4 were negatively correlated with innate immune cells such as mast cells, dendritic cells, and M1 macrophages, but positively correlated with M2 macrophages, neutrophils, and NK cells. Conversely, LGALS3BP exhibited opposite correlations. All five genes were strongly associated with adaptive immune cells, including B and T cells. Notably, all five genes showed significant associations with M2 macrophages, with TFPI and LGALS3BP displaying the strongest correlations, while PDK1 showed a strong correlation with $CD4^+$ memory T cells(Figure 6D). These findings suggest that these genes may participate in inflammatory and immune regulatory processes.

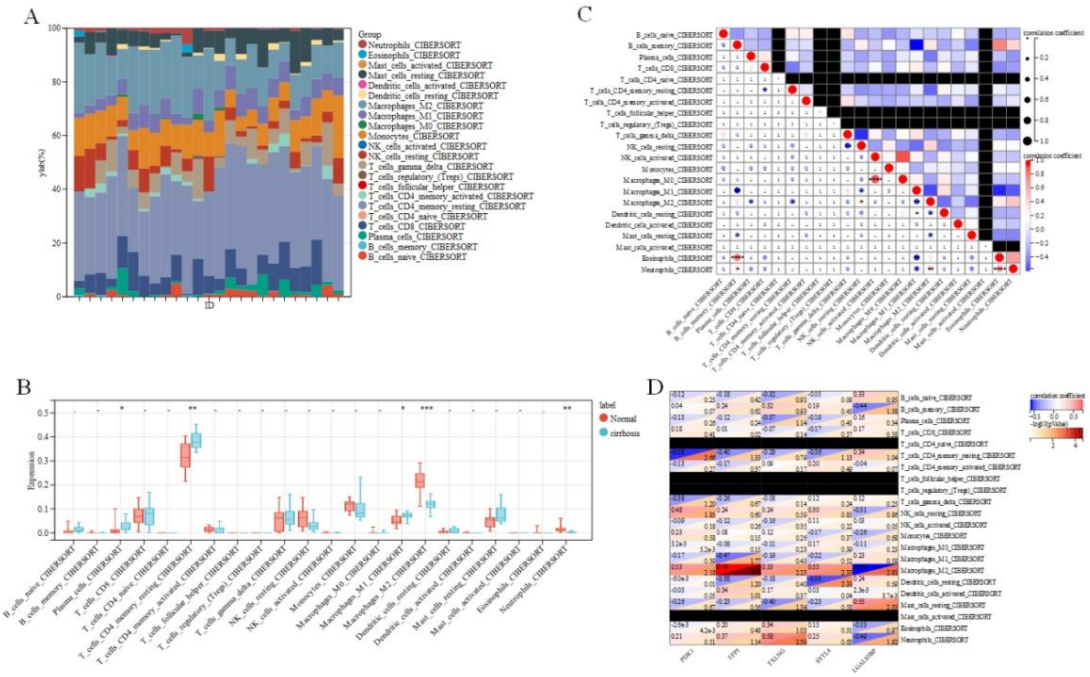


Figure 6. Immune Cell Infiltration Analysis

(A) Stacked bar chart showing proportions of 22 immune cell types in each sample.

(B) Boxplots showing differences in the composition of 22 immune cell subtypes.

(C) Correlation heatmap comparing immune cell proportions between cirrhosis and control groups.

(D) Heatmap showing correlations between target gene expression and immune cell subtypes (red = positive correlation; blue = negative correlation).(*， $P < 0.05$, **， $P < 0.01$, ***， $P < 0.001$).

7. Validation of Target Gene Expression Consistency

qRT-PCR of paraffin-embedded liver tissues from cirrhotic patients with thrombocytopenia (platelet count < 50 × 10^9/L) showed decreased mRNA expression of PDK1, TFPI, TXLNG, and SYTL4, but increased expression of LGALS3BP, consistent with the bioinformatics predictions ($P < 0.05$, Figure 7A).Immunohistochemistry of cirrhotic and non-cirrhotic tissues revealed enhanced expression and granule accumulation of LGALS3BP in cirrhosis (Figures 7B–E). No significant difference was observed between peri-tumoral cirrhotic and non-tumorous cirrhotic tissues (Figures 7F, H), while LGALS3BP expression was markedly reduced in hepatocellular carcinoma (HCC) tissues (Figures 7G, I).

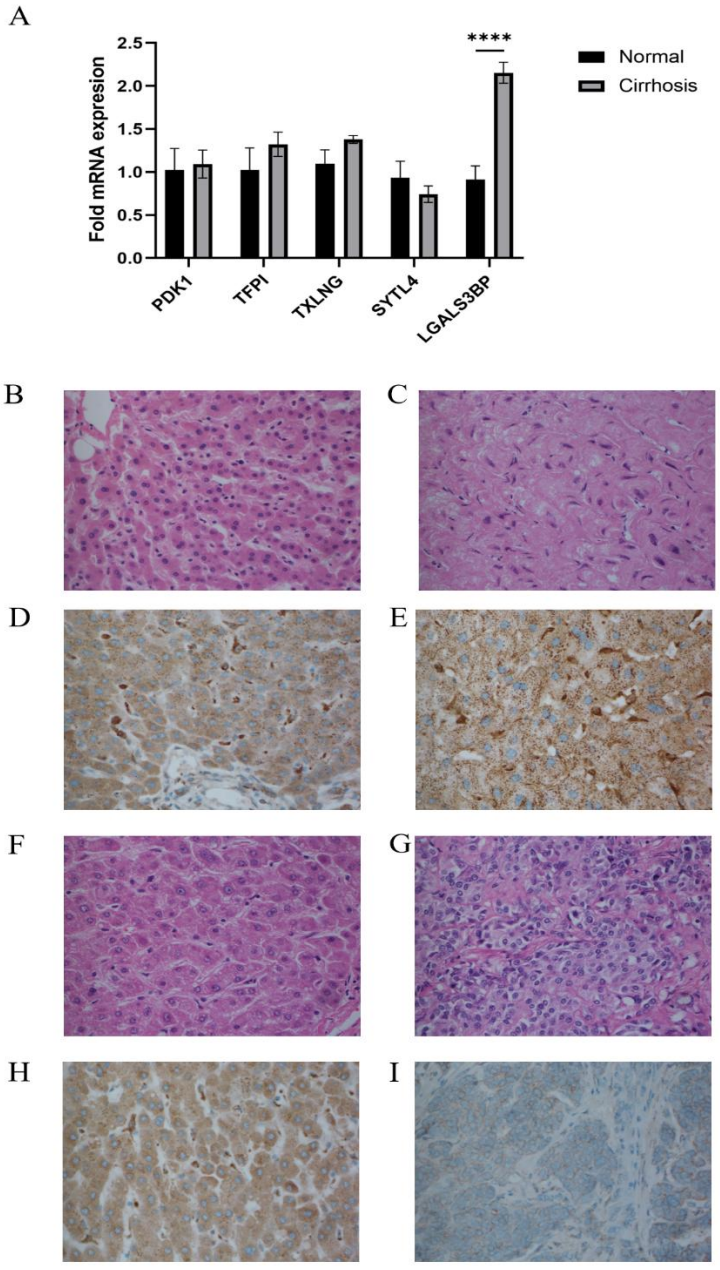


Figure 7. Validation of mRNA and Protein Expression

(A) qRT-PCR analysis of mRNA expression.

(B) Normal liver (HE).

(C) Cirrhotic liver (HE).

(D) Normal liver (IHC).

(E) Cirrhotic liver (IHC).

(F) Peri-tumoral cirrhosis (HE).

(G) Hepatocellular carcinoma (HE).

(H) Peri-tumoral cirrhosis (IHC).

(I) Hepatocellular carcinoma (IHC).

Discussion

During hepatic fibrosis, hepatic stellate cells (HSCs) are activated and play a pivotal role in extracellular matrix (ECM) production [3]. Although fibrosis is reversible, continuous injury without intervention ultimately leads to liver cirrhosis, the major cause of morbidity and mortality among patients with chronic liver disease. Cirrhosis markedly increases the risk of developing hepatocellular carcinoma (HCC) [4]. Despite ongoing experimental exploration of antifibrotic drugs [5], few have achieved clinical success. Hence, elucidating the pathogenesis of cirrhosis and identifying novel therapeutic targets remain critical.

Platelets are essential for hemostasis and play key roles in the progression of hepatic fibrosis, with both platelet count and function changing as liver disease advances [6]. Mechanisms of thrombocytopenia in cirrhosis include reduced platelet production, increased destruction, and splenic sequestration. Current therapeutic strategies—platelet transfusion, thrombopoietin receptor agonists (TPO-RAs), and splenectomy—have limitations. Repeated transfusions may induce anti-platelet antibodies, while TPO-RAs and transfusions may increase the risk of platelet hyperactivation and thrombosis [7].

Recent studies have demonstrated that platelets act as effector and immune cells, contributing to inflammatory and immune responses [6,8]. They can mediate inflammation in systemic lupus erythematosus (SLE) [9] and promote tumor progression and chemoresistance via direct contact or paracrine signaling [10]. Such bidirectional crosstalk between tumor cells and platelets suggests similar interactions may exist between platelets and hepatic cells in cirrhosis, especially given the liver's rich vascularization and the prevalence of thrombocytopenia in this condition.

However, existing studies have mainly focused on platelet counts, function, and surgical risk in cirrhosis [7,11], with limited exploration of molecular mechanisms involving platelet-related genes. In this study, we used bioinformatics approaches integrating Limma, WGCNA, LASSO-Cox, and Random Forest analyses, as well as PPI network construction, to identify five platelet-related genes (PDK1, TFPI, TXLNG, SYTL4, LGALS3BP) and establish a predictive ROC diagnostic model validated across multiple independent datasets.

Among these, LGALS3BP emerged as the most relevant gene. It was enriched in pathways related to biosynthesis, metabolism, ECM–receptor interaction, lysine degradation, and gap junctions. LGALS3BP correlated positively with mast cells, dendritic cells, and M1 macrophages, but negatively with M2 macrophages, neutrophils, and NK cells, and showed strong associations with adaptive immune cells, including B and T lymphocytes. qRT-PCR and immunohistochemistry

confirmed that LGALS3BP expression was elevated in cirrhotic tissues, consistent with in silico analyses.

LGALS3BP encodes a cysteine-rich scavenger receptor glycoprotein, known to participate in immune surveillance and host defense against pathogens and tumors. It is an interferon-inducible secretory glycoprotein that serves as a ligand for galectins, enhancing cell adhesion and activating proinflammatory signaling pathways [12]. Elevated circulating LGALS3BP levels have been reported in hepatic fibrosis patients [13], and platelets have been shown to release LGALS3BP, which correlates with platelet activation, adhesion, and aggregation [9].
However, its functional role in cirrhosis-associated thrombocytopenia has not been fully elucidated. Our findings provide new molecular insights into the crosstalk between platelets and cirrhotic cells, which may not only enhance diagnostic precision but also aid in identifying novel therapeutic targets aimed at improving cirrhosis outcomes while mitigating thrombocytopenia.

References

1. Kisseleva, T. and D. Brenner, *Molecular and cellular mechanisms of liver fibrosis and its regression.* Nat Rev Gastroenterol Hepatol, 2021. 18(3): p. 151-166.
2. Friedman, S.L. and M. Pinzani, *Hepatic fibrosis 2022: Unmet needs and a blueprint for the future.* Hepatology, 2022. 75(2): p. 473-488.
3. Zhang, R., et al., *LncRNA-SNHG5 mediates activation of hepatic stellate cells by regulating NF2 and Hippo pathway.* Commun Biol, 2024. 7(1): p. 266.
4. Lawal, G., et al., *The Immunology of Hepatocellular Carcinoma.* Vaccines (Basel), 2021. 9(10).
5. Zhao, Y., et al., *Inhibitory effects of Curcumae Radix carbonisata-based carbon dots against liver fibrosis induced by carbon tetrachloride in mice.* Artif Cells Nanomed Biotechnol, 2024. 52(1): p. 23-34.
6. Basili, S., et al., *Platelet Count Does Not Predict Bleeding in Cirrhotic Patients: Results from the PRO-LIVER Study.* Am J Gastroenterol, 2018. 113(3): p. 368-375.
7. Qian, J.D., et al., *Management strategies for chronic liver disease-related thrombocytopenia.* Zhonghua Gan Zang Bing Za Zhi, 2021. 29(9): p. 896-899.
8. Dufeys,C.,et al., *Fibroblasts and platelets: a face-to-face dialogue at the heart of cardiac fibrosis*. Am J Physiol Heart Circ Physiol. 2024 Mar 1;326(3):H655-H669.
9. Bannoudi,H.,et al., *Platelet LGALS3BP as a Mediator of Myeloid*

Inflammation in Systemic Lupus Erythematosus. Arthritis Rheumatol. 2023 May;75(5):711-722.

10. Haemmerle, M., et al., *The Platelet Lifeline to Cancer: Challenges and Opportunities.* Cancer Cell, 2018. 33(6): p. 965-983.

11. Shu,L.,et al., *Glycan-Lectin interactions between platelets and tumor cells drive hematogenous metastasis.* Platelet,2024 Dec;35(1):2315037.

12. Xu, G., et al., *Inducible LGALS3BP/90K activates antiviral innate immune responses by targeting TRAF6 and TRAF3 complex.* PLoS Pathog, 2019. 15(8): p. e1008002.

13. Noro, E., et al., *N-glycan structures of Wisteria floribunda agglutinin-positive Mac2 binding protein in the serum of patients with liver fibrosisdagger.* Glycobiology, 2021. 31(10): p. 1268-1278.

Funding

This research was supported by the National Clinical Specialization Construction Project for the Department of Pathology(Progressive project)(2022YBL-JB-01).

Corresponding authors

Correspondence to Xiaodan Fu.

Ethics declarations

Ethics approval and consent to participate

Patient study was approved by the Ethics Committee of First Affiliated Hospital of Fujian Medical University Hospital (Approval No.:MRCTA,ECFAH of FMU[2022]440) and all written informed consent was obtained for this research. Participates gave informed consent to participate in the study before taking part. All methods were performed in accordance with the relevant guidelines and regulations. Due to the observational nature of this study, clinical trial registration was not conducted.

Data Availability Statement.

Researchers interested in further information are invited to contact the corresponding authors via e-mail to:1002603440@qq.com.

Consent for publication

Not applicable.

Competing interests

The authors declare no competing interests.

Author Contributions Statement

Shanshan Huang wrote the main manuscript text. Shanshan Huang and Xiaodan Fu contributed to study concept,design and supervision. Huinan Lu contributed to acquisition,analysis and interpretation of data.Sampling,Diagnosis and scoring was performed by Yupeng Chen.All authors reviewed the manuscript.